INTERNATIONAL JOURNAL OF CHEMICAL REACTOR ENGINEERING

Volume 6 2008 *Article* A45

Experimental and Numerical Investigation of Natural Convection Heat Transfer in Horizontal Elliptic Annuli

Ramadan Y. Sakr[*] Nabil S. Berbish[†]

Ali A. Abd-Aziz[‡] Abdalla Said Hanafi[**]

[*]Benha University, rsakr85@yahoo.com

[†]Benha University, n11264@yahoo.com

[‡]Benha University, alymech@yahoo.com

[**]Cairo University, hanafi1946@yahoo.com

ISSN 1542-6580

Experimental and Numerical Investigation of Natural Convection Heat Transfer in Horizontal Elliptic Annuli

Ramadan Y. Sakr, Nabil S. Berbish, Ali A. Abd-Aziz, and Abdalla Said Hanafi

Abstract

Experimental and numerical studies for natural convection in two dimensional regions formed by a constant flux heat horizontal elliptic tube concentrically located in a larger, isothermally cooled horizontal cylinder were investigated. Both ends of the annulus are closed. Experiments were carried out for the Rayleigh number based on the equivalent annulus gap length ranges from $1.12x10^7$ up to $4.92x10^7$; the elliptic tube orientation angle varies from 0^o to 90^o and the hydraulic radius ratio, HRR, was 6.4. These experiments were carried out for the axis ratio of an elliptic tube (minor/major=b/c) of 1:3. The numerical simulation for the problem is carried out by using commercial CFD code. The effects of the orientation angle as well as other parameters such as elliptic cylinder axis ratio and hydraulic radius ratio on the flow and heat transfer characteristics are investigated numerically. The numerical simulations covered a range of elliptic tube axis ratios from 0.1 to 0.98 and for the hydraulic radius ratios from 1.5 to 6.4. The results showed that the average Nusselt number increases as the orientation angle of the elliptic cylinder increases from 0^o (the major axis is horizontal) to 90^o (the major axis is vertical) and with the Rayleigh number as well. Also, the average Nusselt number decreases with the increase of the hydraulic radius ratio. An increase up to 1.75 and further increases in the hydraulic radius ratio leads to an increase in the average Nusselt number. The axis ratio of the elliptic cylinder has an insignificant effect on the average Nusselt number. Both the average and local Nusselt number from the experimental results are compared with those obtained from the CFD code.

Both the fluid flow and heat transfer characteristics for different operating and geometric conditions are illustrated velocity vectors and isotherm contours that were obtained from the CFD code. Also, two correlation equations that relate

the average Nusslet number with the Rayleigh number, orientation angle, and hydraulic radius ratio and axis ratio are obtained.

KEYWORDS: natural convection, heat transfer, elliptic cylinders, horizontal annulus

1. INTRODUCTION

The process of natural convection heat transfer in annular space was the subject of many theoretical and experimental studies because of their great importance in many engineering applications. This process is of technological importance in the design of heat exchanger device, solar collectors, nuclear reactor, cooling of electrical and electronic components, underground electric transmission cables using pressurized gas and others. The majority of these studies are related to cylinders, whose cross sections are circular and their walls are maintained at constant temperatures. Mack and Bishop [1] made a study in an annular space ranging between two horizontal concentric cylinders. They employed a power series truncated at the third power of the Rayleigh number to represent the stream function and temperature variables. Their results pertain to radius ratio from 1.15 to 4.15 and Rayleigh number less than or equal to $3x10^3$. Comprehensive review for natural convection heat transfer for concentric cylinders is made by Kuehn and Goldstein [2]. They compared the obtained experimental and numerical results using finite difference method. For natural convection in an annulus, Rayleigh number based on gap-width is normally used to determine if the flow is laminar or turbulent [3]. The transition gap-width Rayleigh number for turbulence is about 10^6, [3-5]. For Rayleigh numbers greater than the transition value, the annulus internal flow conditions are characterized by a turbulent upward moving plume above the inner cylinder and turbulent downward flow against the outer wall [6]. The effect of vertical eccentricity and temperature dependent properties are investigated numerically by Shahraki [7]. Char and Lee [8] studied numerically the effect of maximum density on natural convection of micropolar fluids between horizontal eccentric cylinders.

The increasing interest in developing compact and highly efficient heat exchanger motivated researchers to study heat transfer from tubes of non-circular cross section. Special attention was focused on tubes of elliptic cross section since they found to create less resistance to the cooling fluid which results in less pumping power in case of forced flow. In case of power failure, natural convection becomes the dominant mode of heat transfer. Moreover, the elliptic tube geometry is flexible enough to approach a circular tube when the axis ratio approaches unity and approaches a flat plate when the axis ratio becomes very small.

The problem of free convection heat transfer from horizontal elliptic cylinder placed with its major axis vertical in a fluid of infinite extent is investigated by Bader and Shamsher [9]. Their problem was solved for Rayleigh number varies from 10 to 10^3, Pr=0.7, and the cylinder axis ratio (minor/major) varies from 0.1 to 0.964. Bader [10] studied the effect of elliptic cylinder orientation. The cylinder orientation varies horizontal to vertical major axis while

the axis ratio ranges from 0.4 to 0.98 at two Rayleigh numbers of 10^3 and 10^4. Moawed and Ibrahim [11] investigated experimentally free convection from the inside surface of an open ended elliptic tube heated uniformly. They studied the effect of axis ratio and orientation angle. Their experiments covered range of Rayleigh number from $6.5x10^5$ to $1.13x10^8$, axis ratio (major/minor) from 1.5 to 3.5 and orientation angle from 0^o to 90^o. Laminar, transient, two-dimensional free convection heat transfer from the surface of a horizontal elliptic tube is investigated numerically by Mahfouz and Kocabiyik [12]. The investigation covers a Rayleigh number range up to 10^7. The axis ratio (minor/major) of the elliptic cylinder ranges between 0.05 and 0.998 and Prandtl number ranges between 0.1 and 10. Huang and Mayinger [13] investigated the steady free convection from isothermal elliptic tubes for different axis ratios. The local and the average Nusselt number were reported.

Comparatively, fewer publications were noticed for natural convection in non-circular domain. Lee and Lee [14] attempted to formulate the free convection problem in terms of elliptical coordinates for the symmetrical cases of oblate and prolate elliptical annuli and have performed experiments for this geometry. Elshamy et al. [15] studied numerically the case of horizontal confocal elliptical annulus and developed correlations for the average Nusselt number. Chmaissem el al. [16] simulated the case of natural convection in an annular space, having a horizontal axis bounded by circular and elliptical isothermal cylinders. They used finite element method that utilizes Cartesian coordinates, and vorticity-stream function formulation associated with an iterative technique to solve the matrix system. Cheng and Chao [17] employed the body-fitted curvilinear coordinate transformation method to generate a non staggered curvilinear coordinate system and performed numerical study for some horizontal eccentric elliptical annuli. Djezzar and Daguenet [18] solved Boussinesq equations of laminar thermal and natural convection in the case of two dimensional flow, in annular space between two confocal elliptic cylinders. They developed a new calculation code that utilizes the finite volumes with the primitive functions velocity-pressure formulation. The effect of Rayleigh number and the system inclination is investigated for Pr=0.7. Mota et al. [22] studied numerically natural convection heat transfer in a horizontal eccentric elliptic annuli containing saturated porous medium. They solved two-dimensional Darcy-Boussinesq equations n generalized orthogonal coordinates, using high order compact finite differences on a very fine grid.

In the present work, several experimental runs were carried out to show the effect of Rayleigh number and the orientation angle of the heated elliptic cylinder placed in an isothermal cooled circular cylinder. Also, these results are extended through the numerical simulation of the present problem to investigate

the effect of Rayleigh number, orientation angle, axis ratio of the elliptic tube and the hydraulic radius ratio between the circular and elliptic cylinders.

2. EXPERIMENTAL SET UP

The experimental set up used in the present study is shown schematically in Fig. (1). The test section mainly consists of three main parts; the heating system, the cooling system, and the measuring system. Two concentric horizontal cylinders are used to form an annular region. The outer cooling circular cylinder was made from a copper of 200 mm outer diameter, 2 mm thickness, and 300 mm length. The inner heating elliptic cylinder was made of beech wood (high smooth surfaces) with a major diameter (c) of 45 mm and length of 300 mm that had an axis ratio (b/c) 1:3 and give a hydraulic radius ratio (R_o/R_i) of 6.4 with respect to the outer cylinder. A special mechanism is used to maintain a certain angle of orientation for inner elliptic cylinder that varies from 0^o (major axis is horizontal) to 90^o (major axis is vertical). Figure (2) shows the two concentric cylinders and the thermocouples distributions on the surface of the outer, inner cylinders, and annulus. The inner elliptic cylinder is heated at constant heat flux by an electric heating element. A nickel-chrome tape of 0.2 mm thickness and 4 mm width and a resistance 14 Ω is wound helically around the wooden tested elliptic cylinder with a pitch of 1 mm; this provided the condition of approximately constant heat flux. Figure (3) shows the construction of the heating elliptic cylinder. Sixteen pre-calibrated copper-constantan thermocouples (0.4 mm wire diameter) were distributed circumferentially and embedded at the back of the nickel-chrome heater tape at mid-span distance to measure the surface temperature of the inner elliptic cylinder. The inner surface of the outer cooling cylinder is kept at a constant surface temperature (low temperature) by using a circulating water system which is pumped through a wounded coil (with a pitch 0.5 mm) on the outer cylinder surface by a pump of 0.5 hp from a reservoir as shown in Fig. (1). Cooling system consists of a copper coil of diameter 12.5 mm and 15 m length. Four thermocouples are distributed in the wall of the outer cylinder surface as shown in Fig. (2). Eighteens thermocouples are used to measure the temperatures distribution through the annulus between the two cylinders by insertion fixed thermocouple probes from eight plugs located at mid-span distance. Another three thermocouples are used to measure the temperature of inlet and outlet cooling water and to measure the ambient air temperature. The readings of the thermocouples are taken by means of a digital thermometer with an accuracy of 0.1 ^oC. The steady-state condition is achieved after 3 to 4 hours approximately. To confirm a uniform temperature distribution, three thermocouples are installed at the two ends and at mid span of the tested cylinder to measure the axial temperature. The input electric power to the inner cylinder is controlled by means

of a voltage regulator. Five various values of Rayleigh number based on the equivalent annulus gap length were utilized in the experiments which ranged from $1.12x10^7$ to $4.92x10^7$.

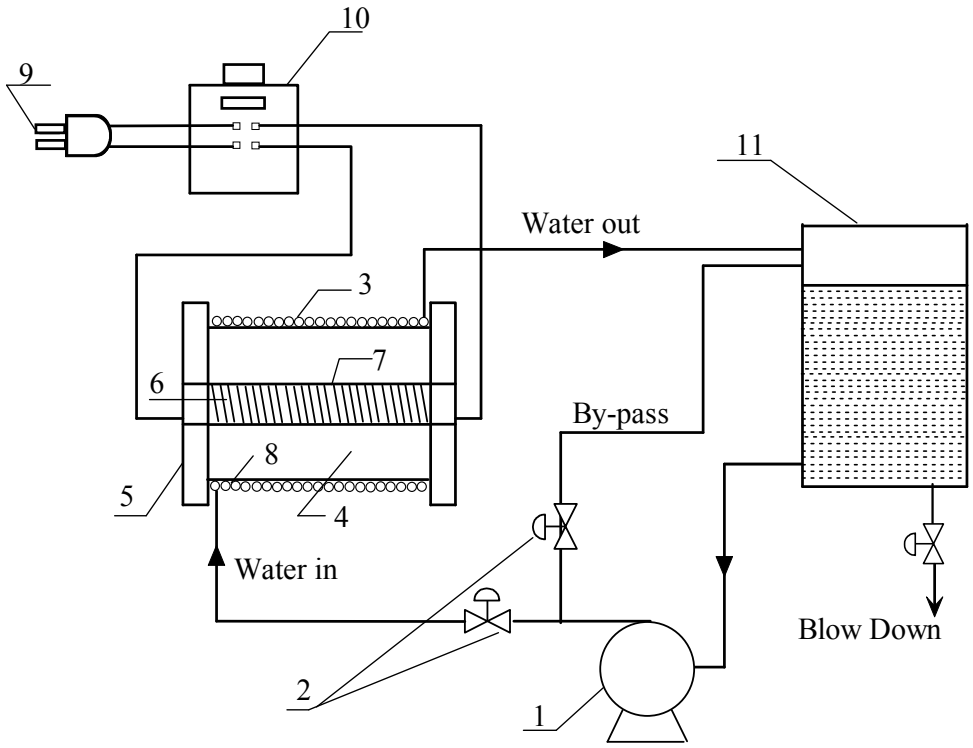

1- Pump	2-Two-way valves	3- Cooling coil
4- Air (Annulus region)	5- Wooden end	6- Heater
7- Inner elliptic tube	8-outer circular cylinder	9- To power supply
10-Voltage regulator	11- Water tank	

Fig. (1) Schematic diagram of the experimental setup

The local heat transfer coefficient, h_x, and the local Nusselt number, Nu_{local}, are calculated, as follows:

$$h_x = \frac{q_H}{(T_x - T_c)} \quad (1)$$

$$Nu_{local} = (h_x L / k) \quad (2)$$

Where; q_H, T_x, T_c, L and k are the net heat flux, local surface temperature, cold wall temperature, equivalent annulus gap length and the air thermal conductivity, respectively. Error analysis including the temperature measurements and fluid properties show that the average Nusselt number has uncertainty of 4.5% and the Rayleigh number is uncertain by up to 6% of the reported values.

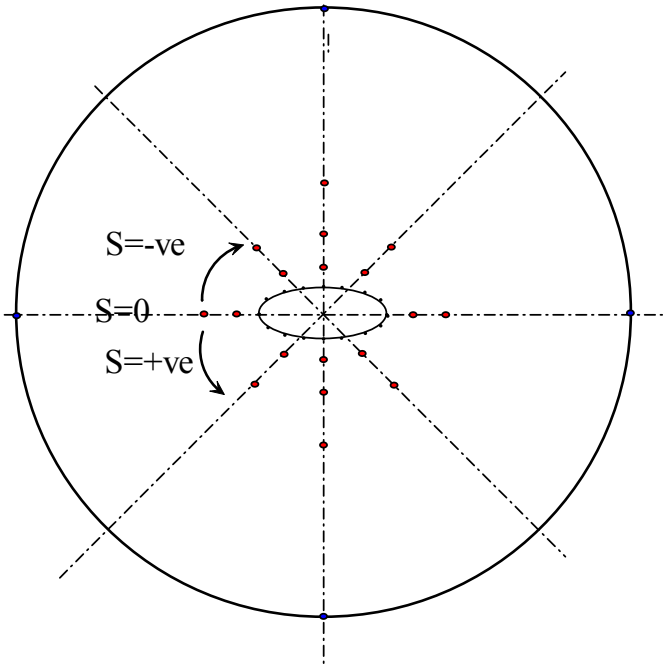

Fig. (2) Thermocouples locations and test section arrangement

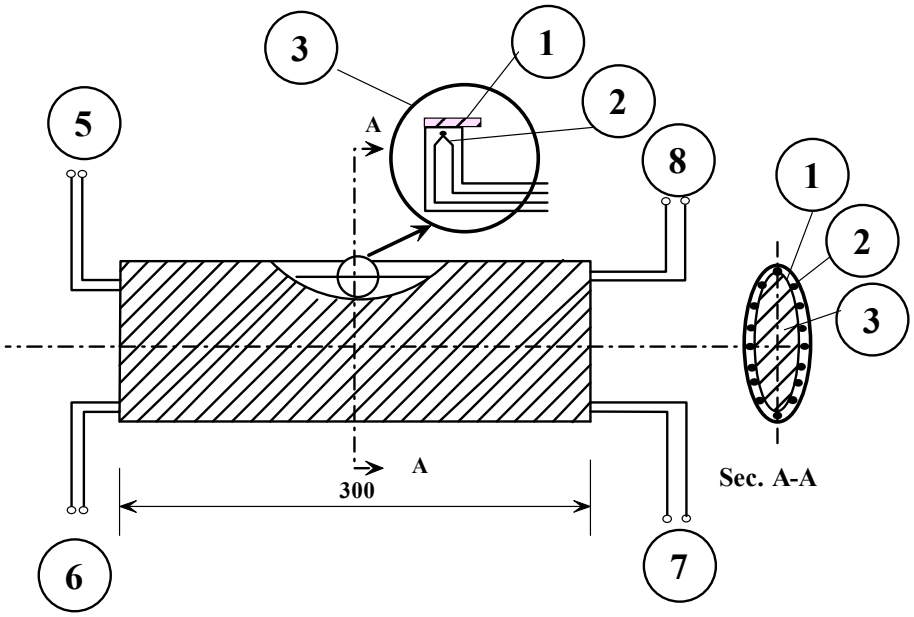

1- Nickel-Chrome tape 2- Thermocouple junction 3- Wooden elliptic cylinder
4- Heating element 5- Thermocouple leads 6- A.C. Power leads
7- Thermocouple leads 8- A.C. Power leads

Fig. (3): Details of heated elliptic cylinder

3. PROBLEM FORMULATION AND BASIC EQUATIONS

Let us consider an annular space ranging from an elliptic cylinder placed at the center of a circular cylinder filled with air. The internal wall of the annular space (elliptic cylinder surface) is heated under constant heat flux q_H, and the external wall of the annular space (circular cylinder surface) is cooled isothermally at temperature T_c. The inner elliptic cylinder is allowed to be inclined to the horizontal axis by an orientation angle; θ. The physical model of the present problem is illustrated in Fig. (4a). The physical properties of air are constant except the air density, where its variations are the origin of natural convection flow. Also, Bousinessq approximation is valid. The present problem is governed by steady, two dimensional equations of continuity, momentum and energy. These equations can be written in the form:

Continuity equation

$$\frac{\partial u}{\partial x}+\frac{\partial v}{\partial y}=0 \tag{3}$$

Momentum equation

$$u\frac{\partial u}{\partial x}+v\frac{\partial u}{\partial y}=-\frac{1}{\rho}\frac{\partial p}{\partial x}+\nu\left(\frac{\partial^2 u}{\partial x^2}+\frac{\partial^2 u}{\partial y^2}\right) \tag{4a}$$

$$u\frac{\partial v}{\partial x}+v\frac{\partial v}{\partial y}=g\beta(T-T_o)-\frac{1}{\rho}\frac{\partial p}{\partial y}+\nu\left(\frac{\partial^2 v}{\partial x^2}+\frac{\partial^2 v}{\partial y^2}\right) \tag{4b}$$

Energy equation

$$\rho c_p\left(u\frac{\partial T}{\partial x}+v\frac{\partial T}{\partial y}\right)=k\left(\frac{\partial^2 T}{\partial x^2}+\frac{\partial^2 T}{\partial y^2}\right) \tag{5}$$

With the boundary conditions applied on the surfaces of both elliptic and circular cylinders respectively as:

$$k\frac{\partial T}{\partial n}=-q_H \tag{6}$$

$$T=T_c \tag{7}$$

4. NUMERICAL APPROACH AND PROCEDURES

In the present experimental work, Rayleigh number based on the equivalent annulus gap length ($L=R_o-R_i$), ranges from $1.12\text{x}10^7$ to $4.92\text{x}10^7$. So, the flow can be considered near the transition condition; $Ra_L=10^6$, [3]. Thus both laminar and turbulent models are used to show which model is best in predicting the natural convection flow inside the considered domain. From the preliminary results of these trials, it was found that the turbulent models can predict the flow field but the temperature field did not show the thermal plume that characterize the thermal field above the heated elliptic cylinder. So, the laminar model is chosen in the present work. Fluent numerical code, version 6.2 is employed for all numerical simulations. Gambit 2.2.30 is used for the development of the computational grid.

Figure (4b) shows the computational grid. The computational domain resulted from the subtraction of the elliptical cylinder section from the circular cylinder section. The grid is made up of triangular elements to improve the quality of the numerical prediction near the curved surfaces. A total number of about 8850 nodes are employed for the entire flow domain to attain grid independent solutions.

Steady, laminar, model is employed to solve natural convection heat transfer. Because Boussinseq air flow is incompressible, continuity is satisfied using a semi-implicit method for pressure linked equations, which is referred to as the SIMPLE procedure. To reduce numerical errors, second order upwind discretization schemes are used in the calculations.

Each computational iteration is solved implicitly. The convergence of the computational solution is determined on scaled residuals for the continuity, energy equations and for many of the predicted variables. The total residual for a given variable is based on the imbalance in an equation for conservation of that variable summed over all computational cells. The settings for the scaled residuals for solution convergence are set to 10^{-3} for nearly all computed residuals. The only exception is the residual for the energy equation which is set 10^{-6}. The solution is considered to be converged when all of the scaled residuals are less than or equal to these default settings. Less than 500 iterations are generally needed for convergence.

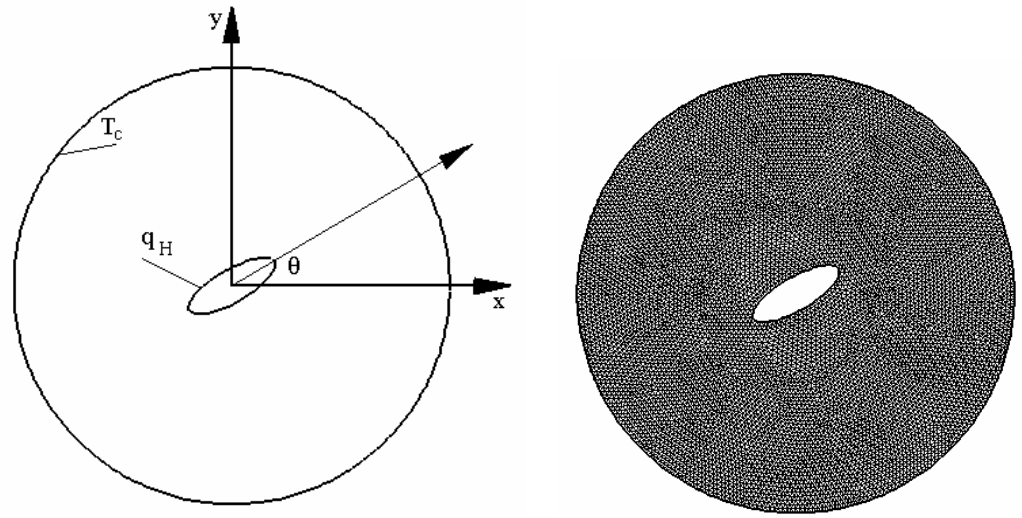

(a) (b)

Fig. (4) Physical domain and computational grid

5. RESULTS AND DISCUSSIONS

5.1. Effect of Orientation Angle

In the present work, the orientation angle which is the inclination angle of the major axis of the heated elliptic cylinder to the horizontal direction varies from 0^o to 90^o. The experimental results that shown in Fig. (5); illustrate the variation of

the average Nusselt number, Nu, with the orientation angle for elliptic tube axis ratio; (b/c=1:3) and hydraulic radius ratio; HRR=6.4. The figure shows that as the orientation angle increases the average Nusselt number increases. Also, the local Nusselt number, Nu_{local} along the heated elliptic cylinder circumference corresponding to $-1.046 \leq S/c \leq 1.046$, is depicted in Figs. (6a-d). The figure is starting from the point of the elliptic cylinder where (S/c=-1.046) and moving in the anticlockwise direction to the point where (S/c=0) and moving in the same direction to (S/c=1.046) for different orientation angles at different Rayleigh numbers based on the equivalent annular gap length. All figures show the same behavior for the local Nusselt number distribution along the heated elliptic cylinder. For all orientation angles and different Rayleigh numbers the maximum value for the local Nusselt number takes place at S/c=0. Symmetric variation on the both sides of the elliptic cylinder for orientation angle 90^o at different Rayleigh numbers is observed. Except for orientation angle 90^o at different Rayleigh numbers, it is observed that the local Nusselt number on the upper surface, ($-1.046 \leq S/c \leq 0$), of the elliptic tube decrease with the increase of S/c up to a certain value then it increases with the increase of S/c till it reaches to the maximum value at S/c=0 then it gradually decreases on the lower surface, ($0 \leq S/c \leq 1.046$), of the tube.

The effect of the orientation angle on the flow field characteristics and thermal field is illustrated in Fig. (7). It is observed that both the velocity vectors and isotherms contours are symmetric about the major axis of the elliptic cylinder for orientation angle 90^o. A thermal plume above the elliptic cylinder is observed for all inclination angles. Also, it is observed that as the orientation angle increases the temperature level decreases, indicating that more cooling for the elliptic cylinder surface, i.e. higher heat transfer rate with the increasing of the orientation angle.

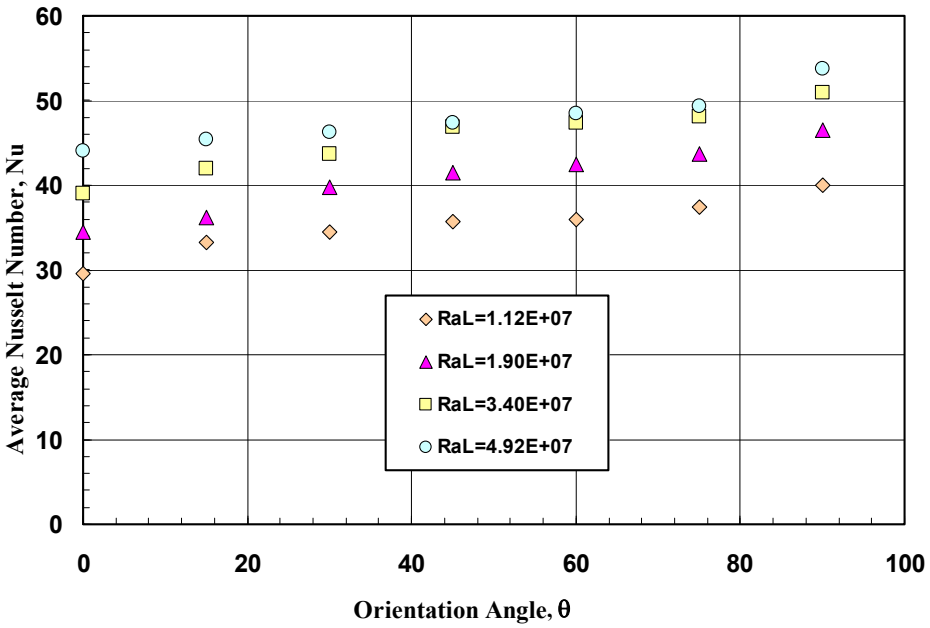

Fig. (5) The variation of the average Nusselt number with the orientation angle for different Rayleigh numbers

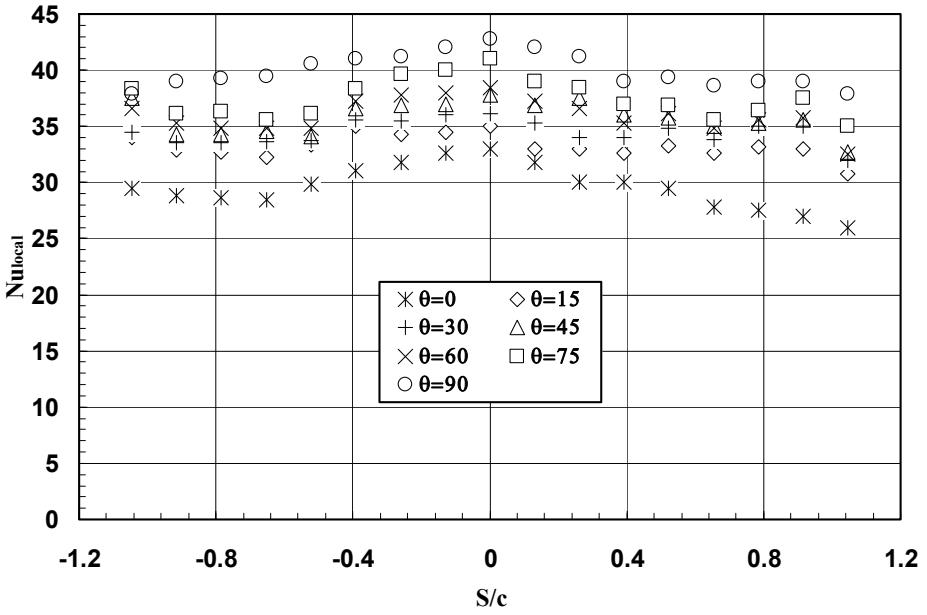

(a) $Ra_L = 1.12 \times 10^7$

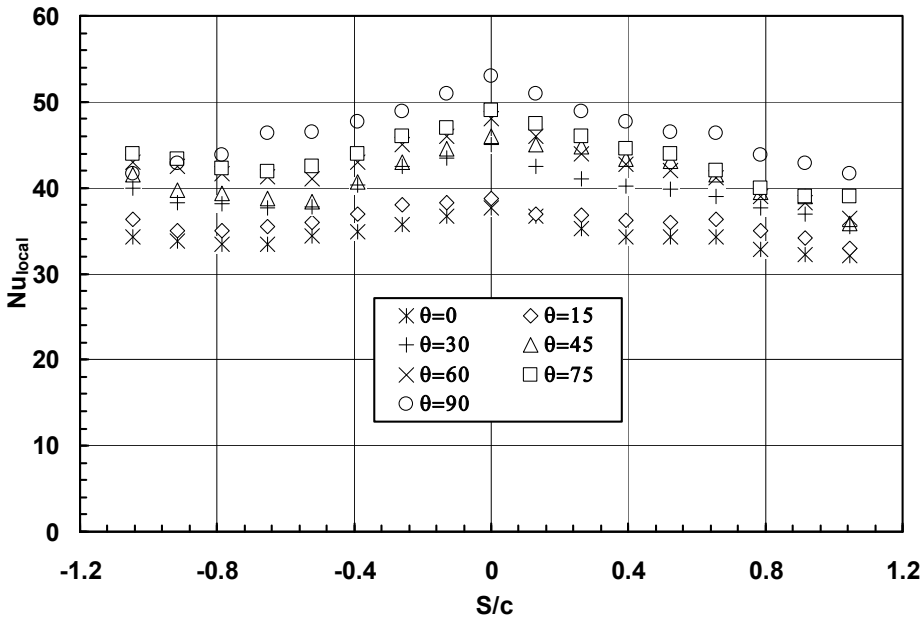

(b) $Ra_L = 1.90 \times 10^7$

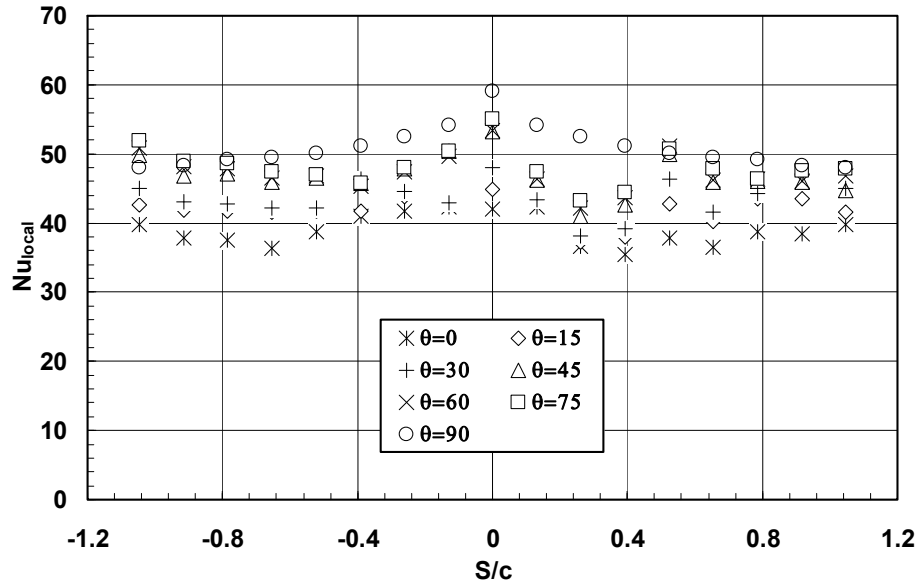

(c) $Ra_L = 3.40 \times 10^7$

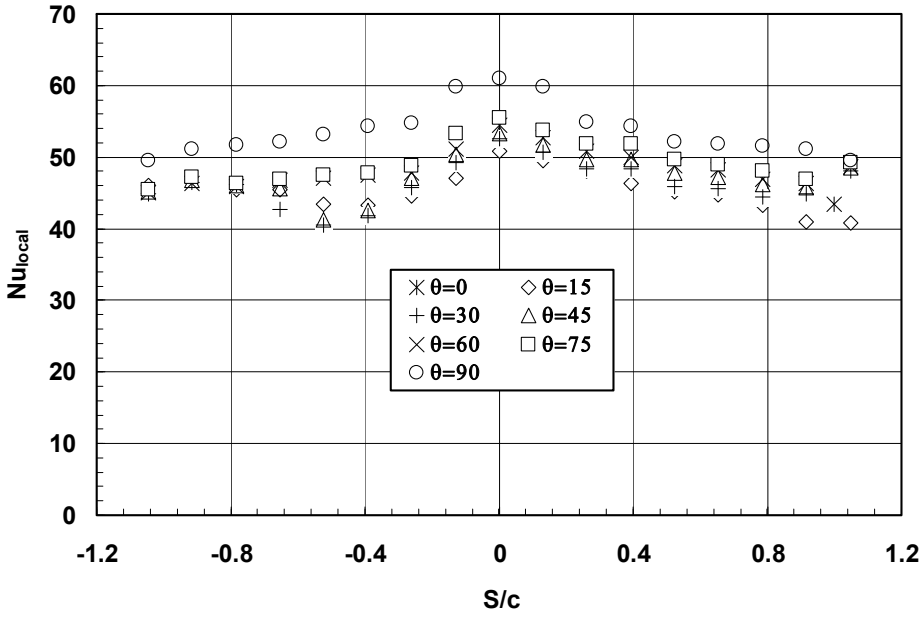

(d) $Ra_L = 4.92 \times 10^7$

Fig (6) The variation of the local Nusselt number along the elliptic cylinder circumference for different orientation angles at different Rayleigh numbers

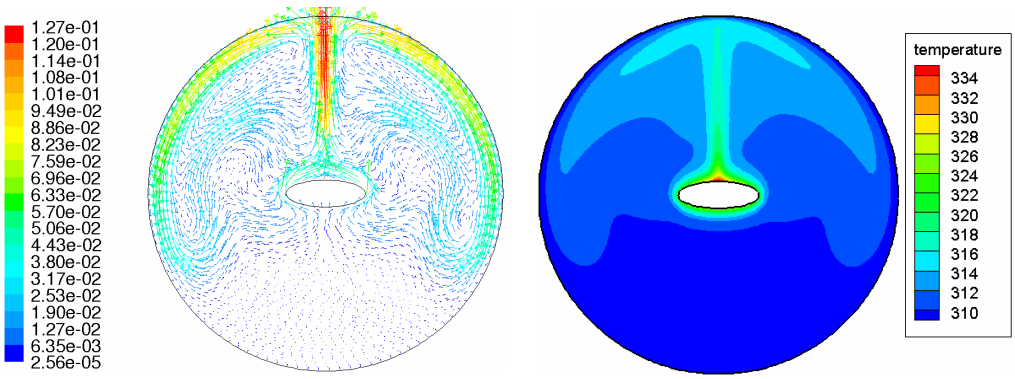

θ = 0

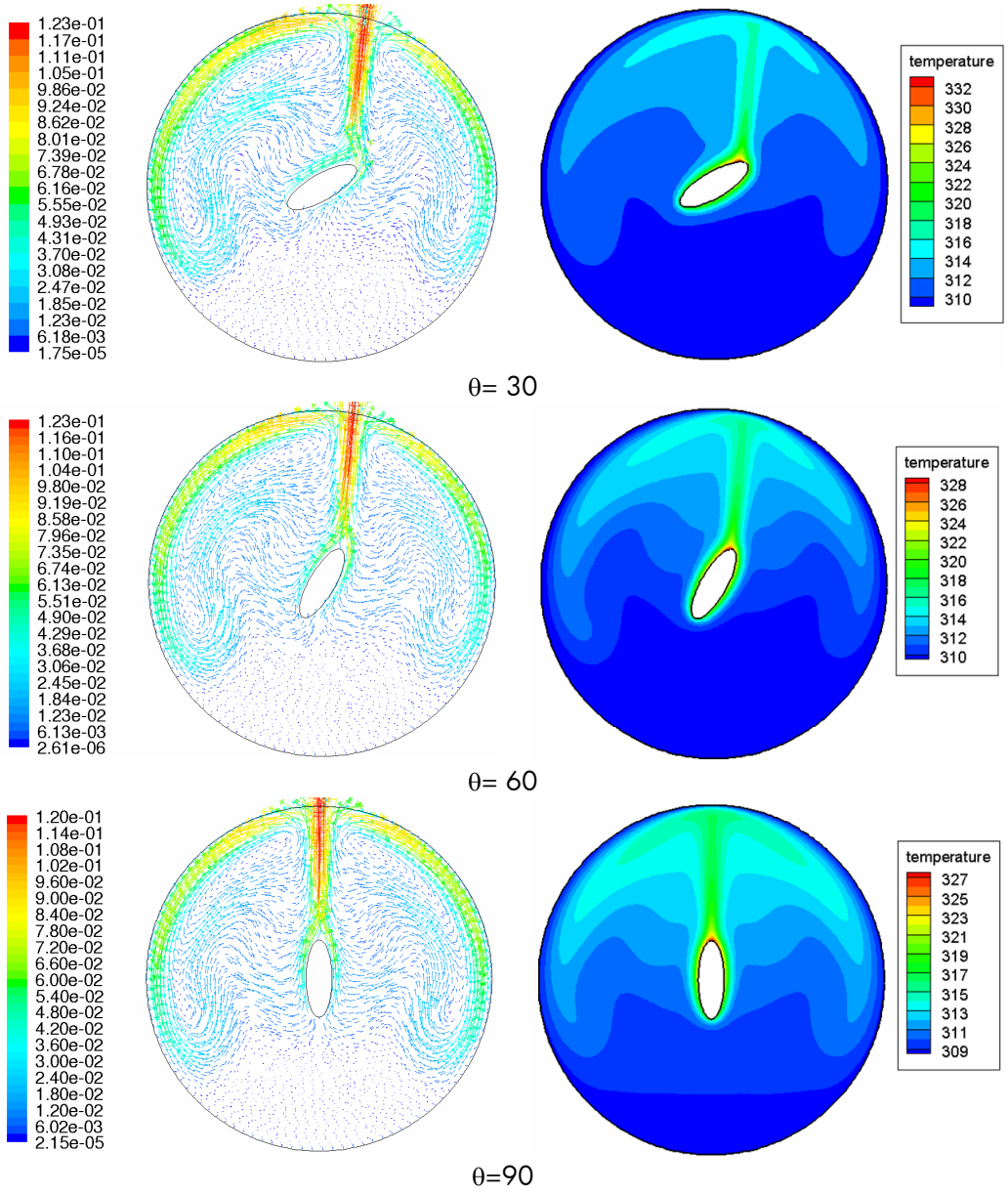

Fig. (7) Velocity vectors (left) and temperature contours (right) for Ra_L=1.12E07, b/c=1:3, HRR=6.4

5.2. Effect of Rayleigh Number

The effect of Rayleigh number based on the equivalent annular gap length Ra_L, on the heat transfer rate represented by the average Nusselt number is illustrated in Fig. (5). The figure shows that Nusselt number increases with the increase of Rayleigh number. The effect of the Rayleigh number on the flow characteristics represented by the velocity vector and heat transfer characteristics represented by isotherms contours for an orientation angle of 90, axis ratio of 1:3 and hydraulic radius ratio of 6.4 is shown in Fig. (8). As stated before, a thermal plume is found above the elliptic cylinder.

5.3. Effect of Hydraulic Radius Ratio

Figure (9) illustrates the effect of the hydraulic radius ratio, HRR in the range of $1.5 \le HRR \le 6.4$ on the rate of heat transfer represented by the average Nusselt number. It is noticed that the average Nusselt number decreases with the increase of the hydraulic radius ratio in the range from 1.5 to 1.75. Then further increase of the hydraulic radius ratio leads to increase in the average Nusselt number for different Rayleigh numbers based on the equivalent hydraulic radius of the elliptic cylinder. This is may be attributed to the longer path of the air fluid layer with higher velocity at higher hydraulic radius ratio. This can be depicted from the velocity vector and isotherms contours illustrated in Fig. (10) for HRR=2 and 6.4 at orientation angle of 90^o , axis ratio of 1:3 and Rayleigh number based on the hydraulic radius of the elliptic tube of 5.57×10^4.

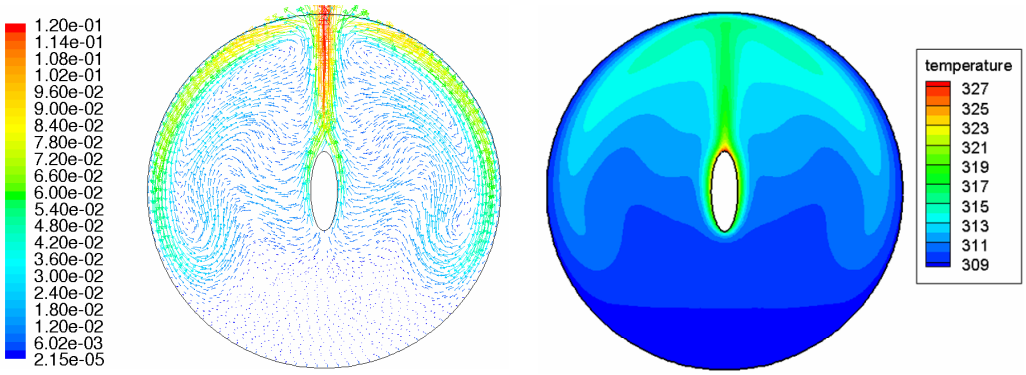

Ra_L=1.12E07

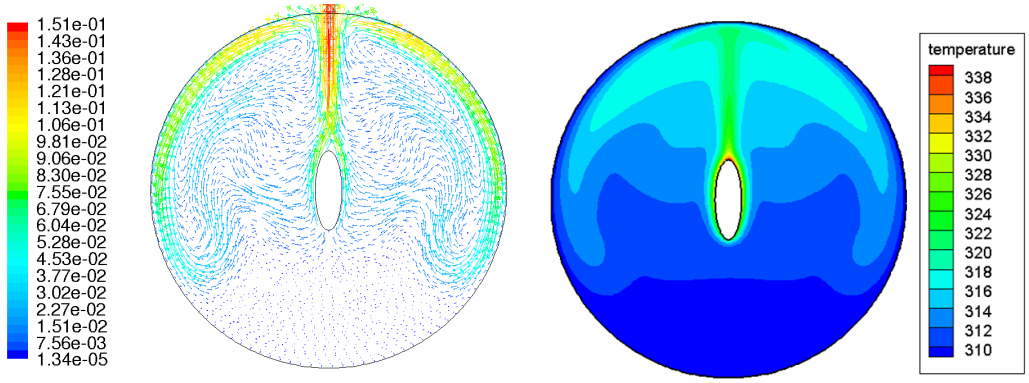

Ra_L=1.90E07

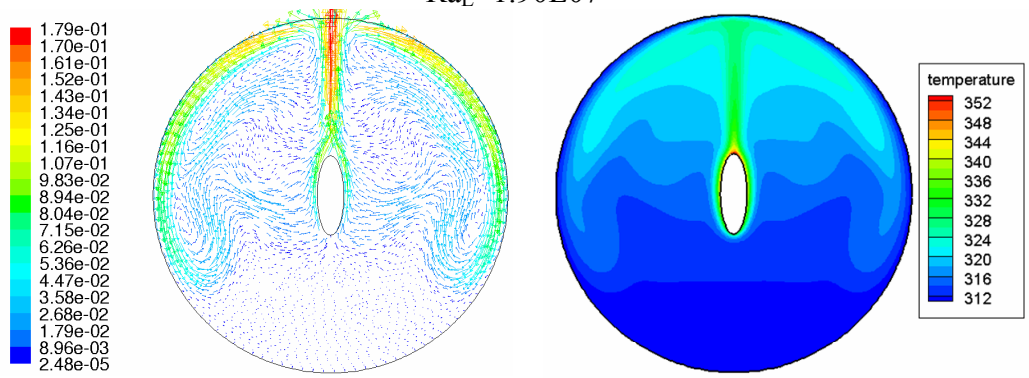

Ra_L=3.40E07

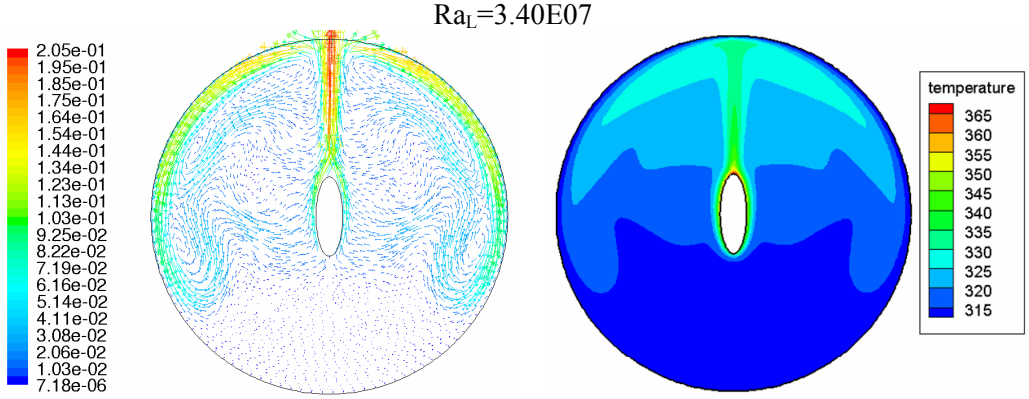

Ra_L=4.92E07

Fig. (8) Velocity vectors (left) and temperature contours (right) for θ=90^o, b/c=1:3, HRR=6.4

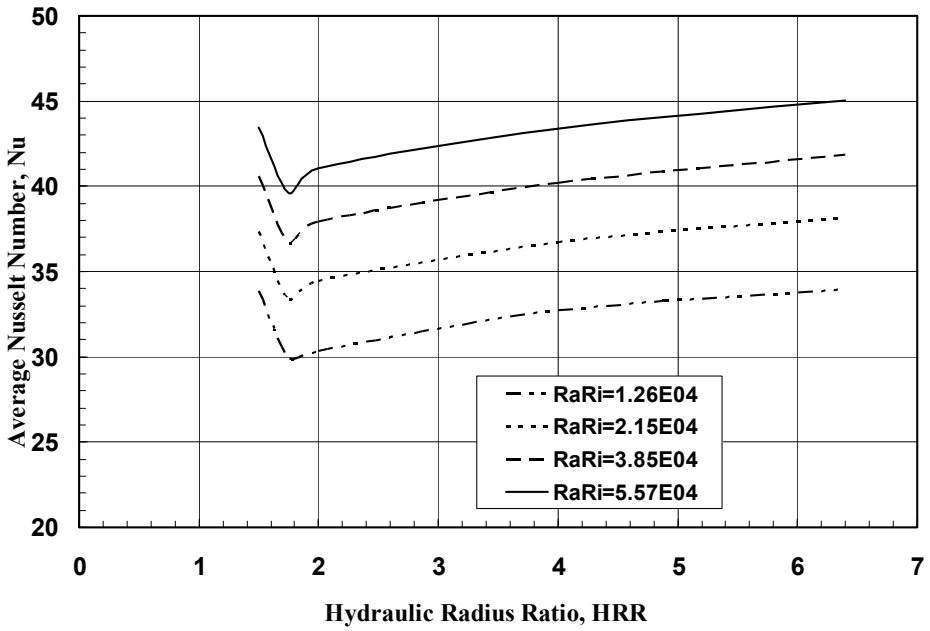

Fig. (9) The variation of the average Nusselt number with hydraulic radius ratio for different Rayleigh number

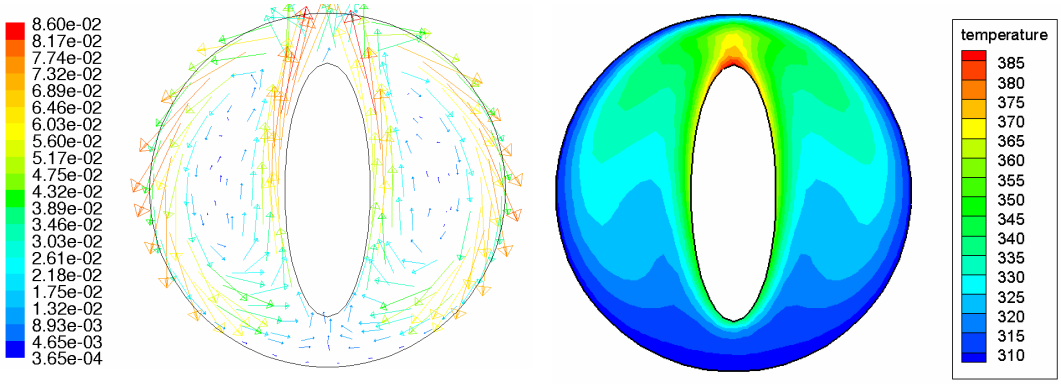

HRR=2

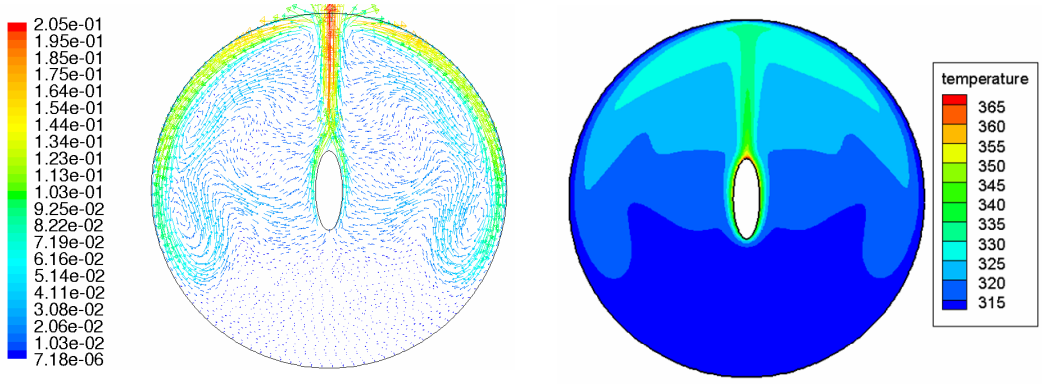

HRR=6.4

Fig. (10) Velocity vectors (left) and temperature contours (right) for θ=90°, b/c=1:3, and $Ra_{Ri}=5.57x10^4$

5.4. Effect of Axis Ratio

The axis ratio of the elliptic cylinder has insignificant effect on the average Nusselt number for any Rayleigh number. This is can be observed from Fig. (11).

5.5. Comparison of CFD Results with Experimental Data

The CFD numerical results for the average Nusselt number for different orientation angles of the elliptic cylinder in the range given by $0^o \le \theta \le 90^o$ at different Rayleigh numbers based on the equivalent annular gap length are compared with the experimental ones that obtained from data reduction. This comparison is depicted in Fig. (12) and good agreement was observed. The CFD predictions for the local Nusselt number are compared with the experimental data at different orientation angles for different Rayleigh numbers as illustrated in Fig.(13). Reasonable agreement is observed between CFD predictions with the experimental results. The data in Fig. (12) was utilized to get a correlation equation that relates the average Nusselt number with both Rayleigh number and the orientation angle using the method of least squares as:

$$Nu = 1.23 Ra_L^{0.196} (1 + \sin\theta)^{0.343},\ 1.12x10^7 \le Ra_L \le 4.92x10^7,\ 0^o \le \theta \le 90^o \quad (8)$$

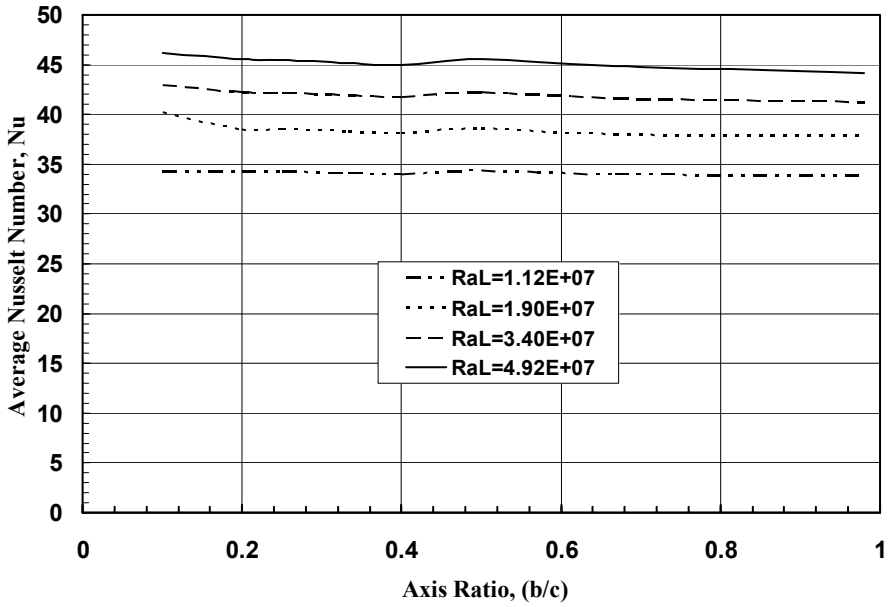

Fig. (11) The variation of the average Nusselt number with elliptic cylinder axis ratio for different Rayleigh numbers

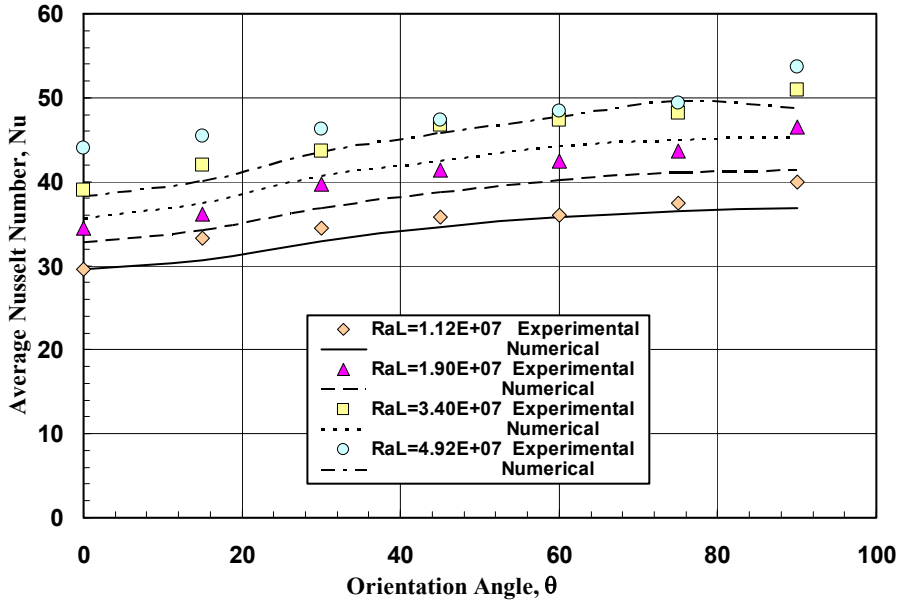

Fig. (12) Comparison between the experimental results with the numerical CFD predictions for the average Nusselt number

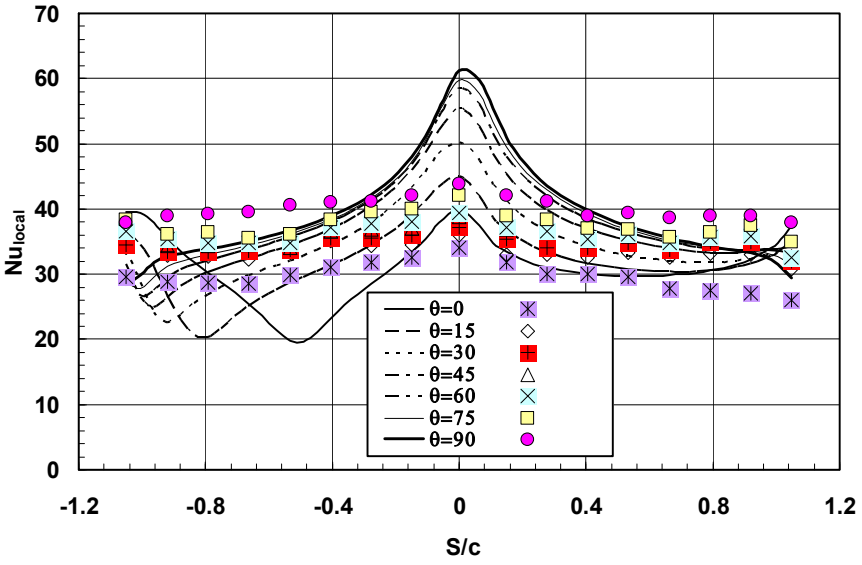

(a) $Ra_L = 1.12 \times 10^7$

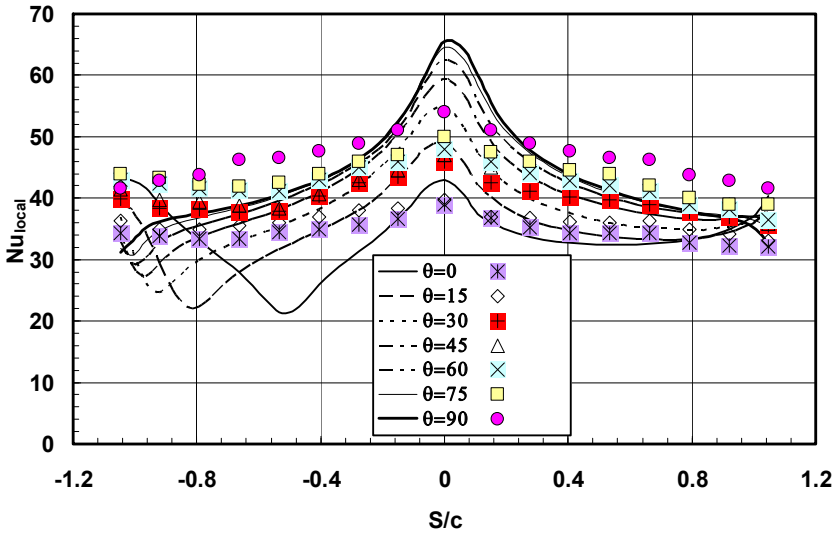

(b) $Ra_L = 1.90 \times 10^7$

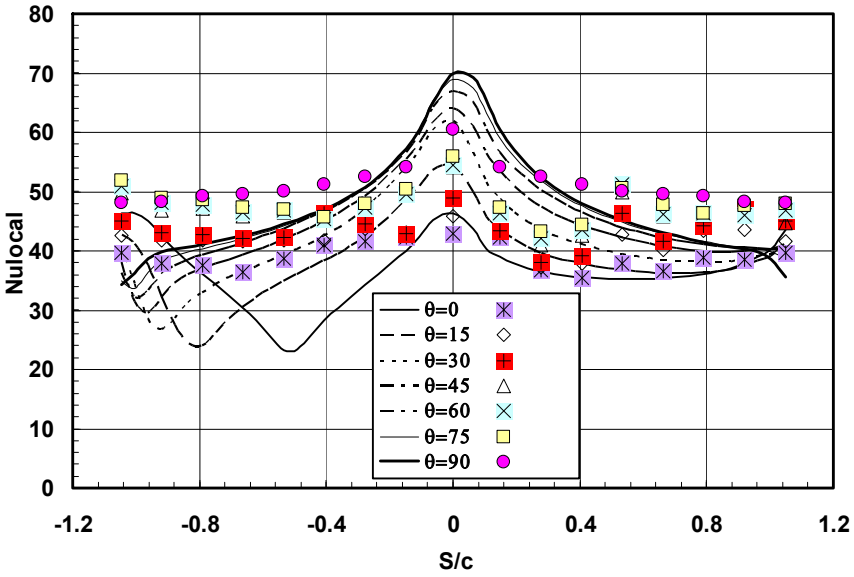

(c) $Ra_L = 3.40 \times 10^7$

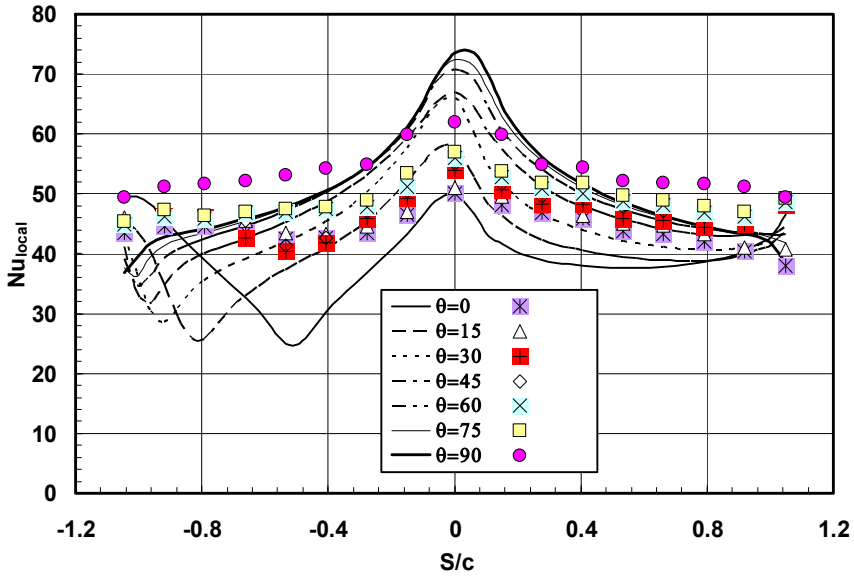

(d) $Ra_L = 4.92 \times 10^7$

Fig (13) CFD predictions for the local Nusselt number variation along the elliptic cylinder circumference for different orientation angles at different Rayleigh numbers

All numerical and experimental data for the average Nusselt number can be represented by the above equation within a maximum error of ±10%. The correlation equation and the experimental data as well as the upper and lower limits are depicted in Fig. (14).

To correlate the average Nusselt number in terms of the other significant variable; HRR, another characteristic length for Rayleigh number should be selected; which in this case is the hydraulic radius of the elliptic cylinder. The following correlation equation is obtained:

$$Nu = 1.264\, Ra_{R_i}^{0.26}\ \mathrm{HRR}^{\ 0.35}(1+\sin\theta)^{0.301}, \qquad (9)$$

$1.26\text{x}10^4 \le Ra_{Ri} \le 5.57\text{x}10^4$, $2.0 \le HRR \le 6.4$, and $0^o \le \theta \le 90^o$

Also, the numerical result that obtained from the CFD code represented as average Nusselt number are also verified through the comparison with other experimental work of Yousefi et. al, [19]. These results are obtained for an elliptic tube having an axis ratio (b/c) of 0.67, with its major axis oriented vertically and for a range of Rayleigh number based on the major axis between 10^3 and $2.5\text{x}10^3$ and their correlation that given by:

$$Nu = 0.56 Ra^{0.25} \qquad (10)$$

As well as the previous works of Merkin et al. [20] and Raithby et al [21], see Fig. (15). This figure shows that the present predictions are in good agreement with the previous works of [19-21].

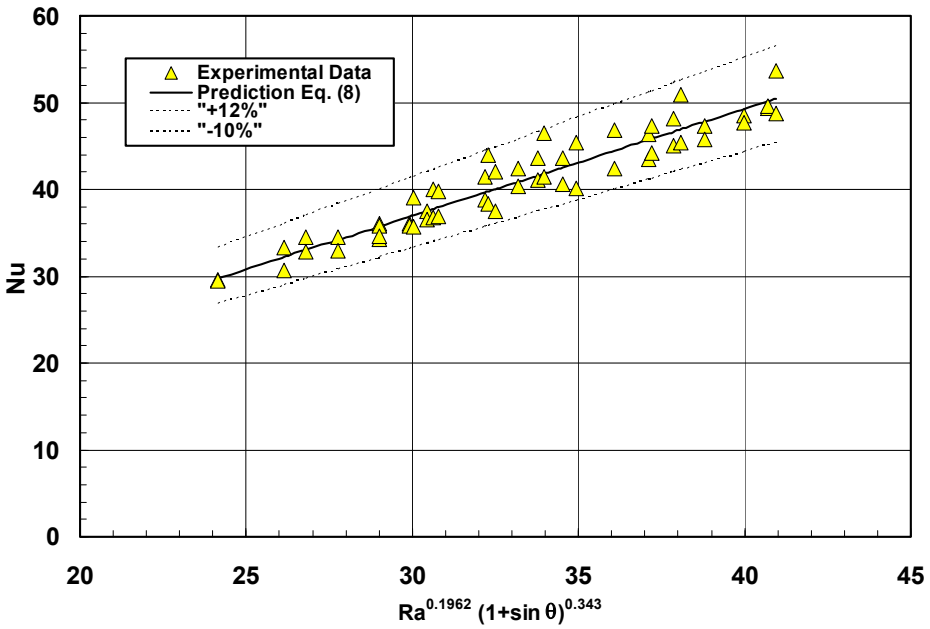

Fig. (14) Presentation of CFD numerical predictions and experimental data

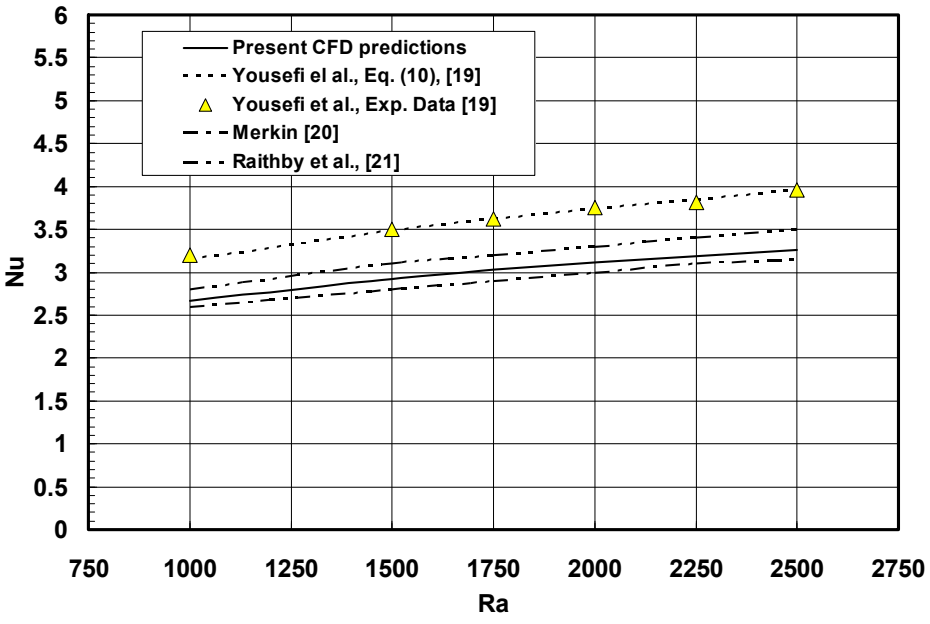

Fig. (15) Comparison between the present CFD numerical predictions with the previous works [19-21].

6-CONCLUSIONS

From the foregoing results that presented in the previous item, the following conclusions can be drawn:

1- The average Nusselt number increases with the increase of the elliptic cylinder orientation angle from the position where its major axis is horizontal to the position of its major axis is vertical.
2- The minimum surface temperature of the heated elliptic cylinder and consequently the maximum local Nusselt located at the lower point of the elliptic cylinder.
3- Both the thermal and velocity fields are symmetric about the major axis of the elliptic cylinder only at an angle of orientation of 90^o, which corresponding to maximum rate of heat transfer condition.
4- The average Nusselt number increases with the increase of Rayleigh number and a correlation equation relating the average Nusselt number with Rayleigh number based on the effective annular gap length and orientation angle is obtained.
5- The average Nusselt number increases with the increase of the hydraulic radius ratio and correlation equation relating the average Nusselt number with Rayleigh number based on the hydraulic radius of the elliptic cylinder, hydraulic radius ratio and orientation angle is deduced.
6- The axis ratio of the elliptic cylinder axis ratio (minor/major, b/c) has insignificant effect on the average Nusselt number.
7- Good agreement between CFD numerical results with the experimental results for the average Nusselt number, but considerable discrepancies were observed for the local Nusselt number which may be due to the slight location discrepancies between them.

NOTATION

b	minor axis length of elliptic cylinder, m
c	major axis length of elliptic cylinder, m
cp	specific heat at constant pressure, J/kg K
d_h	hydraulic diameter, m
h_x	local heat transfer coefficient, $W/m^2.^oC$
HRR	hydraulic radius ratio, R_o/R_i
k	fluid thermal conductivity, $W/m.^oC$
L	equivalent annulus gap length, $L=(R_o-R_i)$, m
Nu_{local}	local Nusselt number
Nu	average Nusselt number

n	normal direction to the surface
p	pressure, Pa
q_H	net heat flux, W/m^2
R_i	inner hydraulic radius, m
R_o	outer hydraulic radius, m
Ra_{Ri}	Rayleigh number based on the inner hydraulic radius
Ra_L	Rayleigh number based on the equivalent annular gap length
S	surface distance from upper point of the elliptic cylinder, taken as negative along the upper side, m
T_x	local surface temperature, ^oC
Tc	cold wall temperature, ^oC
T_o	reference temperature, ^oC
u	x- direction velocity component, m/s
v	y- direction velocity component, m/s
x,y	Cartesian coordinate, m

Greek

β	coefficient of thermal expansion
θ	Orientation angle (angle of attack)
ν	kinematics viscosity, m^2/s
ρ	density, kg/m^3

Subscripts

i	inner
o	outer
c	cold
H	heater

REFERENCES

1- Mack L.R., and Bishop E.H., "Natural Convection between Horizontal Concentric Cylinders for Low Rayleigh Numbers," Q.J. Mech. Appl. Math,, XXI, 1968, pp. 223-241.
2- Kuehn T.H., and Goldstein R.J., "An Experimental and Theoretical Study of Natural Convection in Annulus between Horizontal Concentric Cylinders," J. Fluid Mech., 1976, Vol. 74, pp. 695-719.

3- Kuehn T.H., and Goldstein R.J., "An Experimental and Theoretical Study of Natural Convection Heat Transfer in Concentric and Eccentric Horizontal Cylindrical Annuli," ASME J. of Heat Transfer, 1978, Vol. 100, pp. 1127-1134.
4- Desai C.P., and Vafai, K., "An Investigation and Comparative Analysis of Two- and Three-Dimensional Turbulent Natural Convection in Horizontal Annulus," Int. J. Heat Mass Transfer, 1994, Vol. 37, No. 16, pp. 2475-2504.
5- Char M-I., and Hsu Y-H., "Comparative Analysis of Linear and Nonlinear Low-Reynolds Number Eddy Viscosity Models to Turbulent Natural Convection in Horizontal Cylindrical Annuli," Numerical Heat Transfer, Part A, 1998, Vol. 33, pp. 191-206.
6- Nicholas D.F., Michael T.I., Stephen W.W. and Darryl L.J., "CFD Calculation of Internal Natural Convection in the Annulus between Horizontal Concentric Cylinders," SAND REPORT, 2002, SAND2002-3132.
7- Shahraki F., "Modeling of Buoyancy-Driven Flow and Heat Transfer for Air in a Horizontal Annulus: Effects of Vertical Eccentricity and Temperature Dependent Properties," Numerical Heat Transfer, Part A, 2002, Vol. 42, pp. 603-621.
8- Char M.I., and Lee G.C., "Maximum Density Effects on Natural Convection of Micropolar Fluids between Horizontal Eccentric Cylinders," Int. J. Engng. Sci., 1998, Vol. 36, no. 2, pp. 157-169.
9- Bader H.M., and Shamsher K., "Free Convection from an Elliptic Cylinder with Major Axis Vertical," Int. J. Heat Mass Transfer, 1993, Vol. 36, no. 14, pp.3593-3602.
10- Bader H.M., "Laminar Natural Convection from an Elliptic Tube with Different Orientations," ASME J. of Heat Transfer, 1997, Vol. 119, 709-718.
11- Moawed M. and Ibrahim E., "Heat Transfer by Free Convection inside Horizontal Elliptic Tubes with Different Axis Ratio and different Orientation Angles", Al-Azhar Engineering Ninth International Conference (AEIC), Cairo, Egypt, 2007, April 12-14.
12- Mahfouz F.M. and Kocabiyik S., "Transient Numerical Simulation of Buoyancy Driven Flow Adjacent to an Elliptic Tube," Int. J. of Heat and Fluid Flow, 2003, Vol. 24, pp. 864-873.
13- Huang S.Y., and Mayinger F., "Heat Transfer with Natural Convection around Elliptic Tubes," Wärme und stoffübertragung , 1984, Vol. 18, pp. 175-183.

14- Lee J.H., and Lee T.S., "Natural Convection in the Annuli between Horizontal Confocal Elliptical Cylinders," Int. J. Heat Mass Transfer, 1981, Vol. 24, pp. 1739-1742.
15- Elshamy M.M., Ozisik M.N., and Coulter J.P., "Correlation for Laminar Natural Convection between Confocal Horizontal Elliptical Cylinders," Num. Heat Transfer, Part A, 1990, Vol.18, pp. 95-112.
16- Chmaissem W., Suh S.J., and Daguenet M., "Numerical Study of the Boussinesq Model of Natural Convection in an Annular Space: Having a Horizontal Axis Bounded by Circular and Elliptical Isothermal Cylinder, "Applied Thermal Engineering, 2002, Vol. 22, pp. 1013-1025.
17- Cheng C.H., and Chao C.C., "Numerical Predictions of the Buoyancy-Driven Flow in the Annulus between Horizontal Eccentric Elliptical Cylinders," Num. Heat Transfer, Part A, 1996, Vol. 30, pp. 283-303.
18- Djezzar M., and Daguenet M., "Natural Steady Convection in Space Annulus between Two Elliptic Confocal Ducts: Influence of the Slope Angle," ASME J., 2006, Vol.73, pp. 88-95.
19- Yousefi T., and Ashjaee M., "Experimental Study of Natural Convection Heat Transfer from Vertical array of Isothermal Horizontal Elliptic Cylinders," Experimental Thermal and Fluid Science, 2007, Vol. 32, pp. 240-248.
20- Merkin J.H., "Free Convection Boundary Layer on Cylinders of Elliptic Cross Section," ASME J. Heat Transfer, 1977, Vol. 99, pp. 453-457.
21- Raithby G.D, and Hollands K.G.T., "Laminar and Turbulent Free Convection from Elliptic Cylinders, with a Vertical Plate and Horizontal Circular Cylinder as Special Cases," ASME J. Heat Transfer, 1976, Vol. 98, pp. 72-80.
22- Mota J.P.B, Esteves I.A.A.C, Portugal C.A.M., Esperanca J.M.S.S., and Saatdjian E., “Natural Convection Heat Transfer in Horizontal Eccentric Elliptic Annuli Containing Saturated Porous Media,” Int. J. Heat Mass Transfer, 2000, Vol. 43, pp. 4367-4379.